

Figure 12.4.11 Distribution of Seismic Intensity in MMI Scale

12.4.6 Issues on Ground Motion Estimation

In the analysis of seismic ground motion, several parameters or conditions are assumed in each step under the several restrictions of data and information. Study team believes that many of the restricted situations will be improved with the advance of scientific research in Philippines and more accurate parameters or conditions will be used in near future.

Following is the summary of the technical issues on ground motion estimation analysis.

1) Scenario Earthquakes

- In this study, the magnitude of the scenario earthquakes are estimated from the historical earthquakes or the length of surface fault trace using empirical formula. The trenching study and other geophysical study on the fault can reveal the fault displacement amount at the previous earthquake. The magnitude of the earthquake along the fault can be estimated more accurately by the displacement. If the study on the fault can find the evidence of several historical events, the recurrence interval of the earthquakes and the susceptibility of the next even can be estimated.
- VFS is the largest threats to Metro Manila. Though the existing study shows that recurrence interval in northern area is less than 500 years, the susceptibility of the earthquake along VFS is not clear. The geological, geophysical and paleo-seismological study is necessary.

2) Bedrock Motion Analysis

- The local attenuation formula is not known in Philippines. The suitable existing formula was selected and used in this study but original attenuation formula that reflects the site-specific feature is desirable.
- The seismic motion might have the site-specific characteristics like Casiguran Fault earthquake. The study of strong motion records is desirable.

3) Subsurface Amplification Analysis

- The seismic engineering bedrock of $V_s=700\text{m/sec}$ was adopted as the basement in the analysis of soil amplification analysis. To evaluate the longer period seismic motion, deeper bedrock should be used. The structure prospecting by geophysical technique is necessary.
- The nonlinear property of soil is indispensable to evaluate the large ground motion. The data in Japan was used in this study but the research in Philippines is necessary.
- In this study, the large earthquake motion at just on the fault was evaluated in the case of VFS model. But the evaluation technique at just on the fault is not fixed yet, especially there remains many unsolved issue in evaluating the motion on the sediment layer. The equivalent linear analysis method was used in this study but it is pointed out that this

method has some limitation in applicability to large motion. This issue is not limited to this study or Philippines. This is the big issue in the field of earthquake engineering of the world.

4) Strong Motion Records

- The strong ground motion records are indispensable data to study the issue of earthquake engineering. This is effective to study the attenuation characteristics and site-specific seismic motion characteristics. Observed data is effectively used to validate the ground model. The record of MM-STAR was very effective for this study but it should be pointed out that data is not enough. The station is limited in Metro Manila and this is one of the reasons of the shortage of the strong motion data. The enhancement of strong motion observation network is called for.

References to section 12.4

Abrahamson, N.A. and W.J. Silva, 1997, Empirical Response Spectral Attenuation Relations for Shallow Crustal Earthquakes, *Seism. Res. Lett.*, Vol. 68, No. 1, 94-127.

Annaka, T, F. Yamazaki and F. Katahira, 1997, Proposal of Attenuation Equation for PGA and Sa based on the JMA-87 type accelerogram records, *Proc. 24th Conference on Earthquake Engineering*, 161-164 (in Japanese).

Midorikawa, S., K. Fujimoto and I. Muramatsu, 1999, Correlation of New J.M.A. Instrumental Seismic Intensity with Former J.M.A. Seismic Intensity and Ground Motion Parameters, *Journal of Institute of Social Safety Science*, Vol. 1, 51-56.

Sadigh, K., C.-Y. Chang, J.A. Egan, F. Makdisi and R.R. Youngs, 1997, Attenuation Relationships for Shallow Crustal Earthquakes Based on California Strong Motion Data, *Seism. Res. Lett.*, Vol. 68, No.1, 180-189.

Si, H. and S. Midorikawa, 1999, New Attenuation Relationships for Peak Ground Acceleration and Velocity considering Effects of Fault Type and Site Condition, *Journal of Structural and Construction Engineering (Transactions of AIJ)*, No. 523, 63-70 (in Japanese).

Trifunac M. D. and A. G. Brady, On the Correlation of seismic intensity scales with the peaks of recorded strong ground motion, *B.S.S.A.*, 65, 1975.

Youngs, R, S. Chiou, W. Silva and J. Humphrey, 1997, Strong Ground Motion Attenuation Relationships for Subduction Zone Earthquakes, *Seism. Res. Lett.*, Vol. 68, No.1, 58-74.

12.5 Estimated Tsunami Height

Out of 36 events in the table of earthquake damage in Metro Manila by M.L.P. Bautista(2000), only 2 descriptions about tsunami are found. In 1677, magnitude 7.3 earthquake occur at Manila Trench with 150 km west of Metro Manila. By this earthquake, the west coast of Luzon Island suffered damage by tsunami but there remains no record of damage in present-day Metro Manila. The 1863 earthquake of magnitude 6.5 occurred in Manila Bay. The wave struck the ship and water covered the deck but there are no records of damage on the ground.

As above mentioned, Metro Manila has no experience of damage by tsunami. But if the scenario earthquake of Model 13 or Model 14 may occur at Manila Trench, it is expected that tsunami will attack the coast along Manila Bay. To evaluate the damage by tsunami, the numerical simulation of propagation and run-up of tsunami with bathymetric model from tsunami source region to Metro Manila is necessary. In this study, the run-up height was estimated with simple formula with magnitude and distance from source area. Therefore, the estimated result is not include the effect of the topographical effect of Manila Bay.

12.5.1 Tsunami Height Evaluation Method

The formula by Abe (1989) was used to estimate the tsunami run-up height. Abe (1989) proposed the following formula to estimate the run-up height from earthquake magnitude and propagation distance.

$$\log H_t = M_w - \log \Delta - 5.55 + C \quad \text{----- (7.5.1)}$$

H_t (m) : average run-up height (m) in 20 to 40 km section

M_w : magnitude

Δ : propagation distance of tsunami (km)

C : regional constant

The value $2H_t$ corresponds to the maximum run-up height in the region. Abe (1989) proposed for the value of C based on the experience in Japan that $C=0.0$ for the tsunami that occurred in Pacific Ocean and $C=0.2$ for the tsunami that occurred in Japan Sea.

To confirm the applicability of this formula to Philippines and to decide the value of regional constant C , the observed tsunami height and estimated value by formula (7.5.1) are compared. Two well studied tsunami, namely Aug. 17, 1976 Mindanao Earthquake ($M=7.8$) and Nov. 15, 1994 Mindoro Earthquake ($M_w=7.0$), were used.

The 1976 Mindoro Earthquake occurred in Moro Gulf and tsunami run-up was observed at all around the gulf. Figure 12.5.1 shows the observed run-up height by PAGASA after Nakamura (1977) and estimated value by formula (7.5.1).

The 1994 Mindoro Earthquake occurred in the south of Verde Island Passage. The tsunami was observed at the south coast of Luzon Island and at the north coast of Mindoro Island. Figure 12.5.2 shows the observed run-up height by Imamura et al. (1995) and estimated value by formula (7.5.1).

The observed run-up heights in the figures are the measured or interviewed value at the sight. Therefore, the average of black circle in the section of 20 to 40 km corresponds to the estimated average height that is shown by dashed line, and the maximum height corresponds to the solid line. These figure show that $C=0.2$ leads better correlation between observed and estimated height. In the case of 1994 Mindoro Earthquake, the observed height in Baco Island exceeds the estimated height but the height drastically changes to 1.6 m in the adjacent Baco Media Island. This may be the influence of the energy convergence by round shaped small island (Imamura et al. (1995)). Based on this figure, $C=0.2$ was adopted.

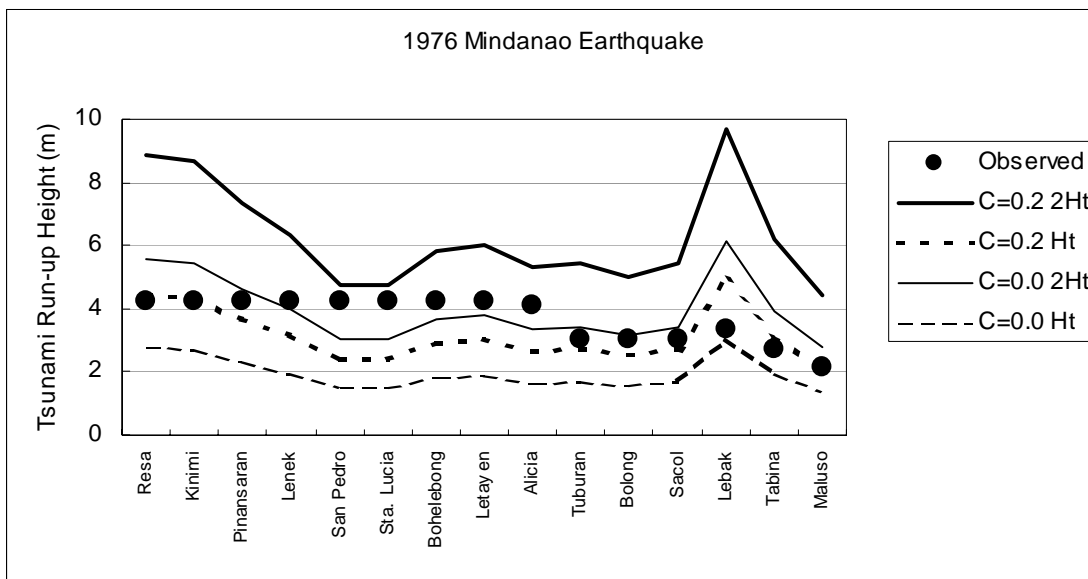


Figure 12.5.1 Observed and estimated run-up height of 1976Mindanao Earthquake

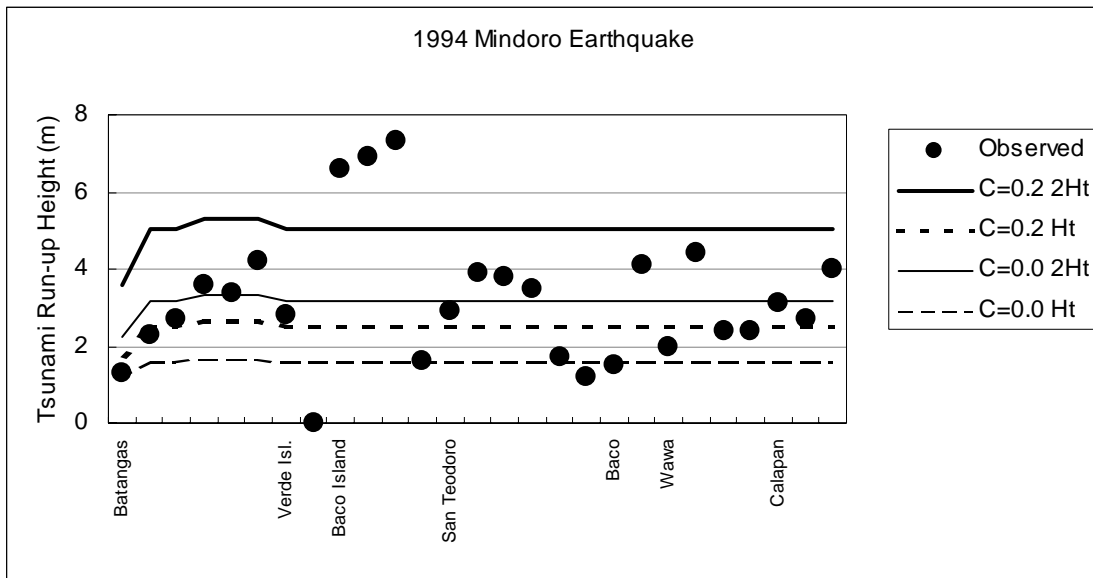


Figure 12.5.2 Observed and estimated run-up height of 1994 Mindoro Earthquake

12.5.2 Estimated Tsunami Height

The location of Model 13 and Model 14 are placed on the subducting Eurasian Plate so as to minimize the shortest distance from Metro Manila to the fault plane. The depth is 40 to 80 km. In general, the shallower earthquake generates larger tsunami wave, therefore, the scenario earthquake for tsunami estimation was considered to occur at Manila Trench in shallow depth. In this condition, the propagation distance from Model 13 and Model 14 is about 200 km in both models. The average run-up height is calculated to be around 1.8 m and the maximum height is around 3.5 m by formula (7.5.1) with $M_w=7.9$ and $C=0.2$.

Next, the arrival time of tsunami was estimated. The propagation speed of tsunami is estimated by following formula.

$$V = \sqrt{g \cdot h} \quad \text{----- (7.5.2)}$$

V : average velocity (m/sec)

g : gravity constant (= 9.8m/sec^2)

h : average depth (m)

The distance from tsunami source area to the mouth of Manila Bay is around 150 km and the average depth is around 2000 m. The distance from the mouth of Manila Bay to the coast of Metro Manila is about 50 km and the average depth is about 25 m. The propagation time from source area to the coast of Metro Manila is about 70 minutes using formula (7.5.2).

In summary, if Model 13 or Model 14 earthquake may occur at Manila Trench, tsunami will attack the coast of Metro Manila around 70 minutes after the earthquake and run-up height will be 2 m in average and may become 4 m in maximum. This assumption is based on the simple estimation method based on the earthquake magnitude and propagation distance. It should be reminded that the effect of islands on the propagation pass and the shape of Manila Bay are not taken into consideration.

The formula (7.5.1) could not be used for Model 18 because this earthquake occurs in Manila Bay. Therefore, the initial tsunami height was calculated by the method of Mansinha and Smylie (1971). This method calculates the vertical ground deformation around the fault in homogeneous and isotropic elastic media. The calculated vertical deformation is usually used as the initial tsunami height for the tsunami propagation numerical simulation. The strike-slip model is supposed for Model 18 in seismic motion estimation. For tsunami estimation, the oblique slip (45 degree) was supposed because pure strike-slip never generates tsunami. The 0.34 m slip was supposed by Wells & Coppersmith (1994). The maximum tsunami height in source area was calculated as 0.12 m. The tsunami height at the coast was evaluated as 0.25 m using Green's theorem;

$H=H_0*(h_0)^{1/4}$, H : tsunami height at the coast, H_0 : tsunami height at off-shore point, h_0 : depth at off-shore point.

In summary, the tsunami by Model 18 will not cause damage to Metro Manila.

References to section 12.5

Abe, K., 1989, Estimate of Tsunami Heights from Magnitudes of Earthquake and Tsunami, Bull. Earthq. Res. Inst., Vol. 64, 51-69 (in Japanese with English abstract).

Bautista, M. L. P., 2000, Destructive Earthquakes that Affected Metro Manila, Philippines from 1589 to 1999, Proceedings of International Workshop on the Integration of Data for Seismic Disaster Mitigation in Metro Manila, November 24-25, 2000.

Imamura, F, E. Gica, H. Lee, C. Synolakis, T. Vasily, E. Listanco, S. Kawashima and D. Esplanada, 1995, On-the-spot Investigation of Mindoro Island, Philippine Earthquake Tsunami, November 15, 1994, Tsunami Engineering Research Report, 12, 19-33 (in Japanese).

Mansinha., L, and D. Smylie, 1971, The Displacement Fields of Inclined Faults, Bull. Seism. Soc. Am., Vol. 61, No. 5, 1433-1440.

Nakamura, S, 1977, The Earthquake and Tsunami in Southern Mindanao, August, 1976, Vol. 15, Southeast Asia Research, No. 1, 95-109 (in Japanese).

Wells, D.L., K.J. Coppersmith, 1994, New Empirical Relationships among Magnitude, Rupture Length, Rupture Width, Rupture Area and Surface Displacement, Bull. Seism. Soc. Am., Vol. 84, No. 4.

12.6 Estimated Liquefaction Potential

12.6.1 General

Metro Manila is divided into three areas depending on topographical feature, as above mentioned in Chapter 12.1. In Coastal Lowland and Marikina Plain, Quaternary deposits with loose sands distributes near ground surface. Liquefaction potential of loose sands is high for large earthquake motion. The liquefaction will cause ground deformation such as subsidence and lateral flow, so that structures will be damaged.

Area ratio of Coastal Lowland and Marikina Plain area to whole Metro Manila area is 34%. In City of Manila, Pasig City and Pateros, lowland area ratio is more than 80%. City of Manila, where capital function concentrates, locates in Coastal Lowland and is substantially vulnerable to liquefaction (Table 12.6.1).

Table 12.6.1 Summary of Quaternary Deposits Distribution by City/Municipality

City/Municipality	Area (ha)	Quaternary Deposits Area (ha)	Area Ratio (%)
Kalookan	53,116	8,526	16
Las Pinas	32,265	2,487	8
Makati	31,961	8,242	26
Malabon	15,962	12,292	77
Mandaluyong	11,069	2,657	24
Manila	41,284	40,441	98
Marikina	22,646	13,569	60
Muntinlupa	38,129	10,896	29
Navotas	10,948	3,041	28
Paranaque	45,606	11,829	26
Pasay	17,779	12,351	69
Pasig	31,883	26,090	82
Pateros	1,951	1,927	99
Quezon	165,330	10,669	6
San Juan	5,880	684	12
Taguig	27,521	17,863	65
Valenzuela	44,518	17,812	40
TOTAL	597,847	201,375	34

Source: Study Team

12.6.2 Analysis Procedure

The following three grades are indicated as the liquefaction potential estimation in the “Manual for Zonation on Seismic Geotechnical Hazards” by TC4, ISSMFE (1993).

Method Grade 1: simple and synthetic analysis by using geological maps, topographical maps and histories of disaster

Method Grade 2: a rather detailed analysis using site reconnaissance results, interviewing the local residents, etc.

Method Grade 3: a detailed analysis using geological investigation results and numerical analyses

It is considered that Method Grade 3 is appropriate in quality and content, compared to other estimation items of the Study. The main content of the evaluation of the liquefaction potential is the comparison of the soil strength with the seismic motion. Various procedures exist to determine these values. Soil properties are determined by simple physical property tests or detailed dynamic laboratory tests. Seismic motion is determined using only information on ground type of the area or an estimated waveform for target earthquakes. In the latter case, the waveform is used to obtain the maximum value of acceleration during an earthquake or time-dependent change of acceleration. The procedure should be determined considering the objective of the estimation. In cases where critical situations are estimated in designing important facilities, a point base analysis is to be used with detailed procedures. In this seismic microzoning study, soil strength and seismic motion are to be determined at the same levels of quality in the whole Study Area. Therefore, using some statistical method is appropriate.

The following information on soil properties and seismic motion was available in the Study:

- Borehole logs with results of Standard Penetration Tests (SPT)
- Physical soil properties
- Peak ground acceleration for scenario earthquakes
- Stress reduction factor

Considering the above, a combination of the F_L method and the P_L method was used in the Study. Procedures are described in next section. This method is commonly used in Japan for practical purposes.

Fill and deposit of soil is the objective of the liquefaction potential analysis. 500m-grid system, which is used in the ground motion analysis, is prepared for modeling. Figure 12.6.1 shows flow chart of liquefaction potential analysis.

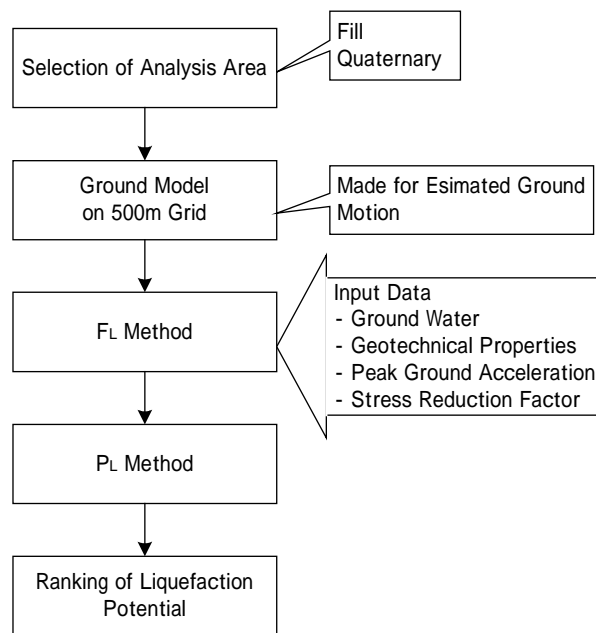


Figure 12.6.1 Flowchart of Liquefaction Analysis

12.6.3 Method of Calculation

The liquefaction potential for individual layers is analyzed by the F_L method. The whole liquefaction potential at the analyzed point is evaluated by the P_L method based upon the results of the F_L method.

F_L Method (Japanese Design Specification of Highway Bridge, revised 1996)

$$F_L = R/L$$

F_L : liquefaction resistance factor

$F_L \leq 1.0$: Judged as liquefied

$F_L > 1.0$: Judged as not liquefied

R: cyclic shear strength at effective overburden pressure

$$R = C_w \times R_L$$

C_w : correlation coefficient for earthquake type

Type 1 earthquake (plate boundary type, large scale)

$$C_w = 1.0$$

Type 2 earthquake (inland type)

$$C_w = 1.0 \quad (R_L \leq 1.0)$$

$$= 3.3R_L + 0.67 \quad (0.1 < R_L \leq 0.4)$$

$$= 2.0 \quad (0.4 < R_L)$$

R_L : cyclic resistance ratio obtained by laboratory test

$$R_L = 0.0882 (N_a/1.7)^{0.5} \quad (N_a < 14)$$

$$= 0.0882 (N_a/1.7)^{0.5} + 1.6 \times 10^{-6} (N_a - 14)^{4.5} \quad (14 \leq N_a)$$

Sandy Soil

$$N_a = c_1 N + c_2$$

$$c_1 = 1 \quad (0\% \leq F_c < 10\%),$$

$$= (F_c + 40) / 50 \quad (10\% \leq F_c < 60\%)$$

$$= F_c / 20 - 1 \quad (60\% \leq F_c)$$

$$c_2 = 0 \quad (0\% \leq F_c < 10\%)$$

$$= (F-10)/18 \quad (10\% \leq F_c)$$

F_c : fine contents

Gravelly Soil

$$N_a = \{1 - 0.36 \log_{10}(D_{50}/2.0)\} N_i$$

N : SPT blow count

N_a : N value correlated for grain size

$$N_i: 1.7N/(\sigma_v' + 0.7)$$

D_{50} : grain diameter of 50% passing (mm)

L : shear stress to the effective overburden pressure

$$L = \alpha / g \times \sigma_v / \sigma_v' \times r_d$$

r_d : stress reduction factor

$$r_d = 1.0 - 0.015x$$

x : depth in meters below the ground surface

α : peak ground acceleration (gal)

g : acceleration of gravity (= 980 gal)

σ_v : total overburden pressure

σ_v' : effective overburden pressure

PL Method (Iwasaki et al. 1982)

$$P_L = \int_0^{20} F \cdot w(z) dz$$

$15 < P_L$ Very high potential

$5 < P_L \leq 15$ Relatively high potential

$0 < P_L \leq 5$ Relatively low potential

$P_L = 0$ Very low potential

$$F = 1 - F_L \quad (F_L < 1.0)$$

$$= 0 \quad (F_L \geq 1.0)$$

$$w(z) = 10 - 0.5z$$

P_L : liquefaction potential index

F_L : liquefaction resistance factor

$w(z)$: weight function for depth

z : depth in meters below the ground surface

12.6.4 Precondition for the Analysis

1) Analyzed Layer

In general, liquefaction occurs in loose saturated sandy deposits. Japanese Design Specification of Highway Bridge defines following soil conditions as required for liquefaction potential evaluation.

In principle, Alluvial saturated sandy deposits, which satisfy following three (3) conditions at a same time, require liquefaction potential analysis.

- 1) Saturated sandy layer above the depth of 20 m from the present ground surface with groundwater level within 10 m from the present ground surface.
- 2) Soil layer with fine contents (F_c) less than 35%, or with plastic index less than 15% even the F_c more than 35%
- 3) Soil layer with mean grain size (D_{50}) less than 10 mm, and with grain size of 10 % passing less than 1 mm.

Liquefaction potential evaluation is recommended for Diluvial deposit with low N value or without diagenesis.

Figure 12.6.2 shows variation of soil properties of D_{50} , D_{10} and F_c by each ground classification. Regarding D_{50} and D_{10} , every ground classification satisfies the requirement for evaluation. F_c , of clayey layer, UC and LC, shows almost more than 35%. Hence, the clayey layer does not satisfy the requirements.

In some soil of fill, sandy layers (US1, US2, US3, LS1, LS2, and LS3) and gravelly layer (LG), F_c value exceeded 35% and PI value shows less than 15 (Figure 12.6.3). Hence, fill, sandy layers and gravelly layers, which appear from the present ground surface to depth 20m, are examined.

2) Geotechnical Properties

Geotechnical properties, such as N value, grain size of 50% passing D_{50} , fine contents F_c and wet density γ_b , are required for analysis of Liquefaction. These are defined for each ground classification. N value of sandy soil of the upper layer slightly increases to depth direction and the N value of the soil was expressed by equations with depth. Data of the Study and existing boring investigation are fully considered. Table 12.6.2 show the summary of the geotechnical properties.

3) Groundwater Level

Data on detail distribution of groundwater table and its seasonal/ tidal change is not available in the Study area. Figure 12.6.4 shows initial groundwater level, those were observed during boring investigation of the Study. Groundwater level shows almost 0.5 to 1.0m and it was rainy season. In the liquefaction calculation, groundwater level was set as 0.5m for all the Study area. This leads to safer side evaluation of liquefaction potential.

4) Peak Ground Acceleration and Stress Reduction Factor

The peak ground acceleration and the stress reduction factor (r_d) were calculated in ground motion analysis for every 500m grid. These values are directly applied.

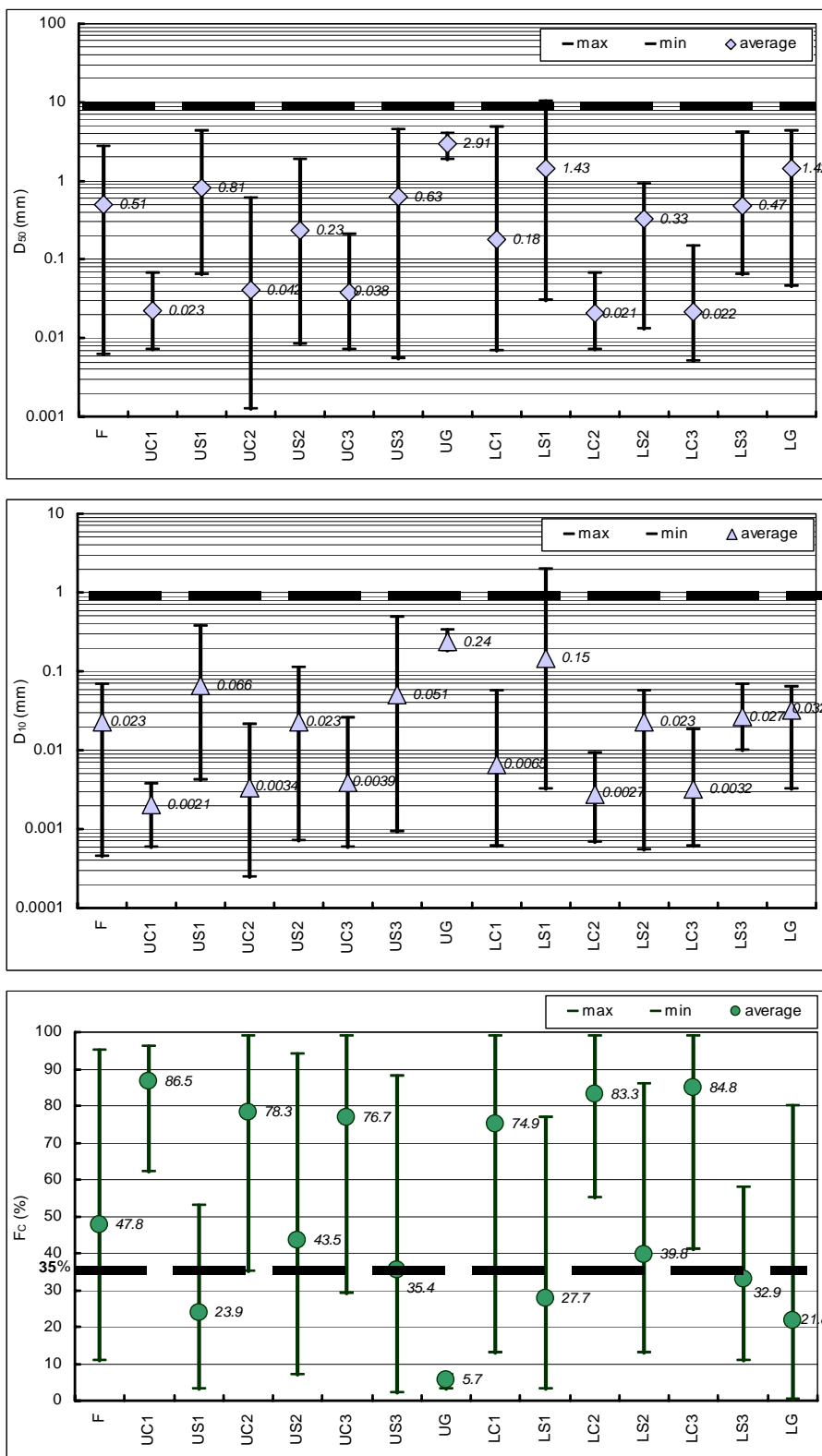


Figure 12.6.2 Variation of Soil Properties, D₅₀, D₁₀ and F_c, for Each Ground Classification

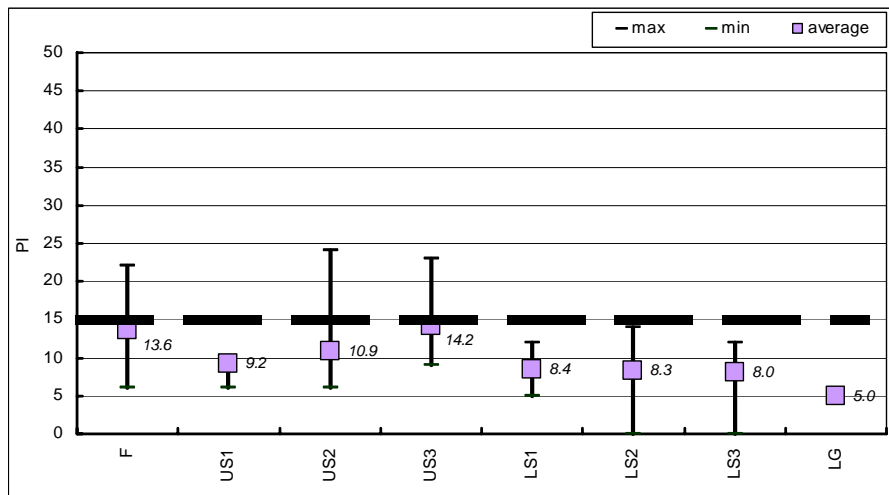


Figure 12.6.3 Variation of Soil Properties, PI, for Each Ground Classification

Table 12.6.2 Summary of Geotechnical Properties for Liquefaction Analysis

Ground Classification	Coastal Lowland				North Part of Marikina Plain				South Part of Marikina Plain				Mutinlupa (Marikina Plain)			
	N (times)	D ₅₀ (mm)	Fc (%)	γ _t (g/cm ³)	N (times)	D ₅₀ (mm)	Fc (%)	γ _t (g/cm ³)	N (times)	D ₅₀ (mm)	Fc (%)	γ _t (g/cm ³)	N (times)	D ₅₀ (mm)	Fc (%)	γ _t (g/cm ³)
F	7	0.61	38	1.75	7	0.61	38	1.75	7	0.61	38	1.75	7	0.61	38	1.75
US1	(d+1 0.9) /1.7	0.22	18	1.74	(d+2 4.2) /1.7	4.4	10	1.81	(d+1 0.6) /1.7	0.69	16	1.90	-	-	-	-
US2	(d+1 7.4) /5.4	0.082	56	1.70	(d+2 7.0) /5.4	0.11	40	1.73	(d+3 9.8) /5.4	0.23	28	1.73	(d+3 9.8) /5.4	0.12	47	1.67
US3	(d+3 5.7) /2.2	0.49	18	1.77	(d+3 5.7) /2.2	0.15	40	1.92	-	-	-	-	(d+3 8.0) /2.2	0.66	21	1.67
UG	24	2.91	6	2.00	24	2.91	6	2.00	24	2.91	6	2.00	24	2.91	6	2.00
LS1	50	1.95	16	1.96	-	-	-	-	39	0.13	38	1.88	49	0.39	32	1.71
LS2	-	-	-	-	-	-	-	-	50	0.39	27	1.75	50	0.51	24	1.75
LS3	-	-	-	-	50	0.31	38	1.86	50	0.27	29	1.82	-	-	-	-
LG	50	2.24	18	2.00	50	2.24	18	2.00	50	2.24	18	2.00	50	2.24	18	2.00

N: N value (≤50)

D₅₀: Grain Size of 50% passing

Fc: Fine Contents

γ_t: Wet Density

d: Depth (m)

-: No Data

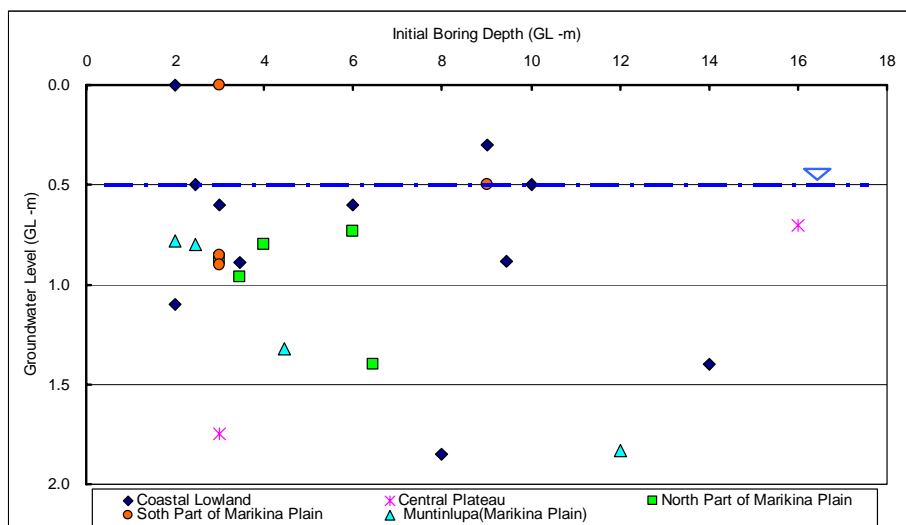


Figure 12.6.4 Observed Groundwater Level in the Study

5) Type of Ground Motion

In calculation of F_L value, earthquake type are determined, type 1 or type 2. Type 1 is applied to plate boundary type earthquake. Type 2 is applied to inland type earthquake. Total 18 scenario models were considered in the Study and type of ground motion for liquefaction analysis is determined as shown in Table 12.6.3.

Table 12.6.3 Summary of Type of Ground Motion for Each Scenario Earthquake

No.	Model Name	Tectonic Condition	Type of Ground Motion
1	PFZ:Digdig Segment	Crustal	1
2	PFZ:Infanta Segment	Crustal	1
3	PFZ:Ragay Gulf Segment	Crustal	1
4	Casinguran Fault	Subduction	2
5	E-W Transform Fault	Crustal	1
6	East Luzon Trough	Subduction	2
7,8,9	West Valley Fault	Crustal	1
10	East Valley Fault	Crustal	1
11	Laguna-Banahaw Fault	Crustal	1
12	West Boundary Fault	Crustal	1
13	Manila Trench (16-14N)	Subduction	2
14	Manila Trench (14-12.5N)	Subduction	2
15	East Zambales Fault	Crustal	1
16	Lubang Fault	Crustal	1
17	Central Midoro Fault	Crustal	1
18	1863 Earthquake	Crustal	1

12.6.5 Liquefaction Potential

1) Result of Analysis

Liquefaction potential was evaluated using P_L value (Table 12.6.4)

Table 12.6.4 Criterion for Evaluation of Liquefaction Potential

Liquefaction Potential	Criterion	Explanation
Very high	$15 < P_L$	Ground improvement is indispensable
Relatively high	$5 < P_L \leq 15$	Ground improvement is required Investigation of important structures is indispensable
Relatively low	$0 < P_L \leq 5$	Investigation of important structures is required
Very low	$P_L = 0$	Liquefaction prone area

The results are summarized in Figure 12.6.5 to Figure 12.6.7.

2) Description

The results of liquefaction analysis are described as follows,

- Results of Model 07, 08 and 09 regarding West Valley Fault shows the highest potential of liquefaction as shown in Figure 12.6.5.
- In Model 07, 08, and 09, high liquefaction potential area (shown as red color in Figure 12.6.7) distribute at around mouth of Pasig River (City of Manila), area from center of Pasig City to Pateros or Tguig, part of Marabon, Paranaque City and Marikina City.
- Model 13 and 14 are plate boundary type earthquake. In these models, relatively high liquefaction potential area (shown as yellow color in Figure 12.6.7) distribute at City of Manila and Taguig.
- Model 18 is recurrence of 1986 earthquake, which occurred in Manila bay. In the model, high liquefaction potential area (shown as red color in Figure 12.6.7) distribute around mouth of Pasig River (City of Manila), some part of Marabon and Paranaque City.
- Liquefaction potential in City of Manila, Paranaque City and Taguig show relatively high.

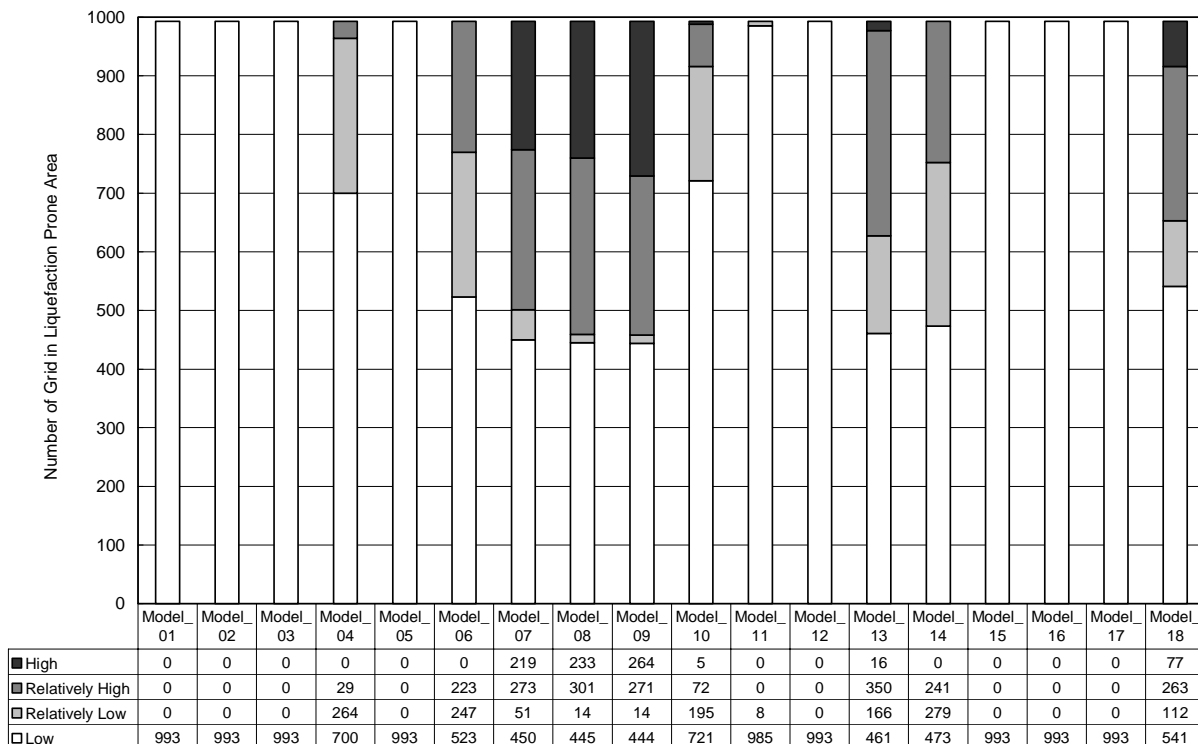


Figure 12.6.5 Results of Liquefaction Analysis for Each Scenario Earthquake

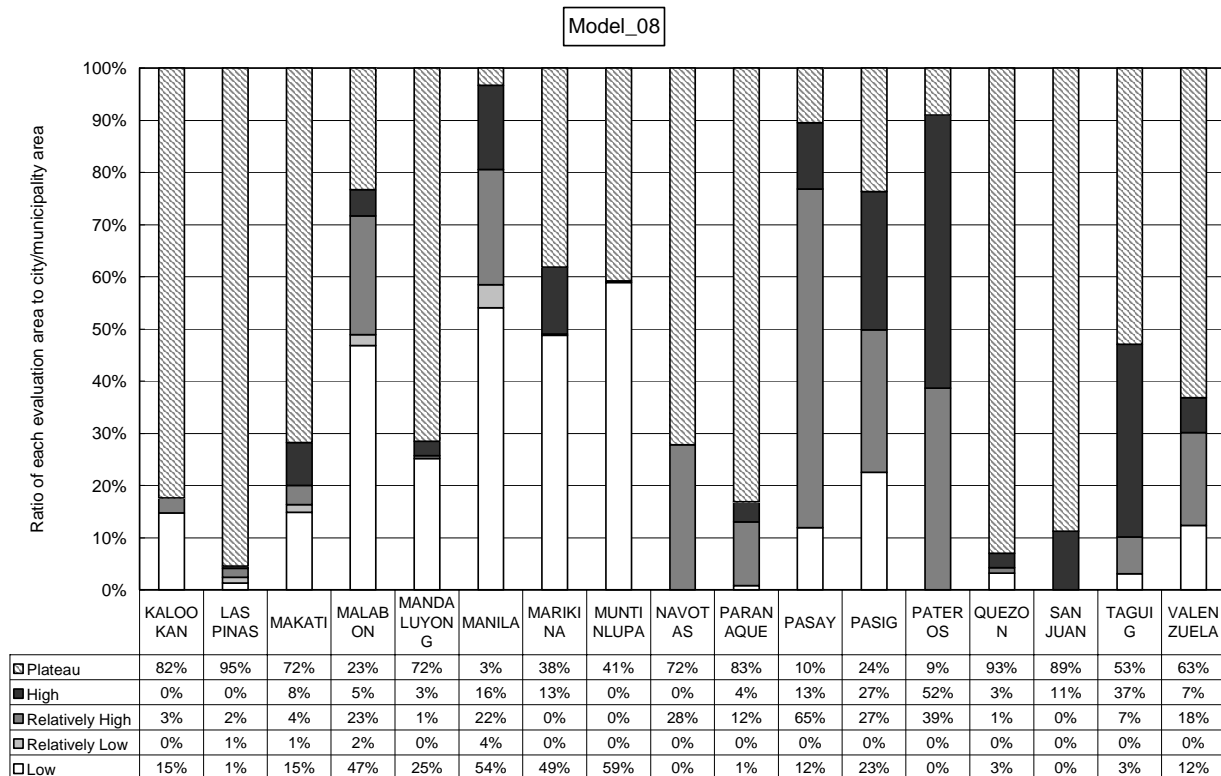


Figure 12.6.6 Variation of Liquefaction Potential in Each City/Municipality, Case of Scenario Earthquake Model 08

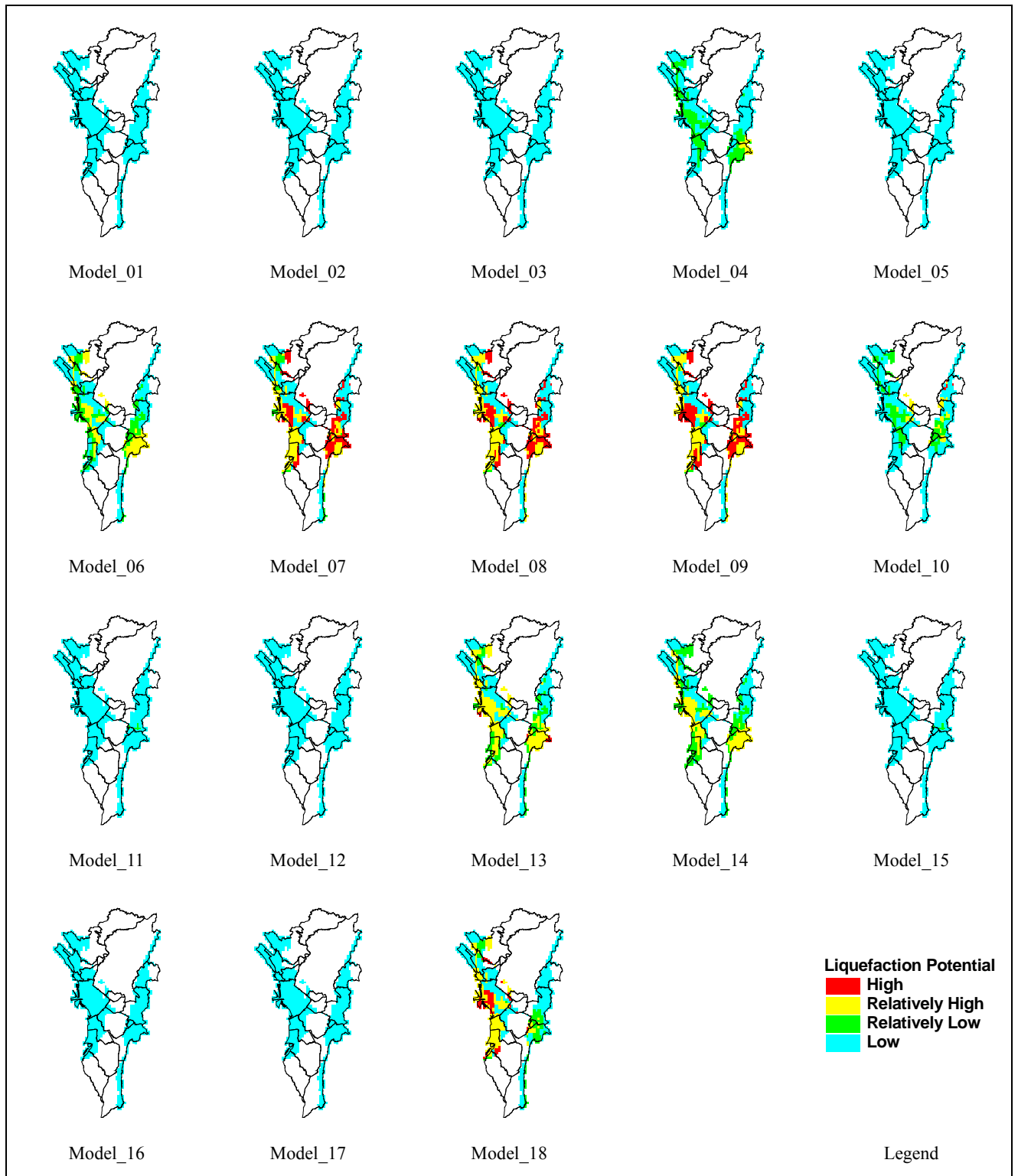


Figure 12.6.7 Liquefaction Potential Map

3) Discussion

Area of high potential for liquefaction does not mean that whole the area will be liquefied during earthquake. This means liquefaction phenomena are observed in many places compared to other

area during earthquake. Also area of low potential for liquefaction does not mean that whole the area will be safe from liquefaction during earthquake. Therefore, in every case, detail evaluation for stability of foundation of important facilities is necessary.

Reference to Section 12.6

ISSMFE, 1993, Manual for Zonation on Seismic Geotechnical Hazards, Technical Committee for Earthquake Geotechnical Engineering, TC4, International Society of Soil Mechanics and Foundation Engineering.

Japan Road Association, 1996, Japanese Design Specification of Highway Bridge (in Japanese).

12.7 Estimated Slope Stability Potential

12.7.1 General

1) Background

Metro Manila is divided into three areas depending on topographical feature, as mentioned in Chapter 12.1. Topographical feature of Central Plateau is gentle in general and steep slopes distribute only at alongside of West Valley Fault and East Valley Fault, in north part of Quezon City and in south part of Muntinlupa (Figure 12.1.4) in the Central Plateau area. Area ratio of Central Plateau area to whole Metro Manila area is 66%. In Kalookan City, Las Pinas City, Quezon City and San Juan City, ratio of plateau area to each city/municipality area is more than 80% (Table 12.7.1).

In this section, slope failure, such as surface failure and rock fall and caused by earthquake, are examined.

2) Present Slope Condition

The followings are features of present condition of slopes in the Study area.

In North of Quezon, South of Muntinlupa, natural slope prevails mainly in rural area. Steep slope distribute alongside of stream or rivers (Picture-1). Ground surfaces are often covered with sediments.

Slopes distribute alongside of West Valley Fault. Subdivision areas are developed especially at gentle-gradient slope areas (Picture-2). Informal settlements are prevailing especially steep-gradient slope areas.

Residential buildings are often built at the top of, at the toe of and on slopes, especially alongside of West Valley Fault (Picture-3). Grounds are basically stiff or rigid and open cracks are observed. Outcrop of ground kept without specific protective measures.

There are cut slopes alongside of roads. Outcrop of ground kept without specific protective measures and weathering is often progressing at slope surface (Picture-4).

Major types of slope failure are surface failure and rock fall of relatively small scale (Picture-5 and 6). In case of earthquake induced slope failure, same type of failure is considered to occur.

Table 12.7.1 Summary of Central Plateau Area by City/Municipality

City/Municipality	Area (ha)	Central Plateau Area (ha)	Area Ratio (%)
Kalookan	53,116	44,590	84
Las Pinas	32,265	29,779	92
Makati	31,961	23,719	74
Malabon	15,962	3,670	23
Mandaluyong	11,069	8,412	76
Manila	41,284	843	2
Marikina	22,646	9,077	40
Muntinlupa	38,129	27,233	71
Navotas	10,948	7,907	72
Paranaque	45,606	33,778	74
Pasay	17,779	5,427	31
Pasig	31,883	5,793	18
Pateros	1,951	24	1
Quezon	165,330	154,662	94
San Juan	5,880	5,196	88
Taguig	27,521	9,658	35
Valenzuela	44,518	26,705	60
TOTAL	597,847	396,473	66

Source: Study Team



Picture-1 Steep Slope alongside of Stream



Picture-2 Subdivision Area alongside of West Valley Fault



Picture-3 Multiple Residential Housing on Top of Slope



Picture-4 No Slope Protection Work



Picture-5 Surface Failure



Picture-6 Surface Failure, Distribution of Weathered Zone

12.7.2 Analysis Procedure

1) General Approach

The following three methods are indicated as the slope stability estimation methods in the “Manual for Zonation on Seismic Geotechnical Hazards” by TC4, ISSMFE (1993).

- 1) Method Grade 1: simple and synthetic analysis by using seismic intensity or magnitude without information of geological condition
- 2) Method Grade 2: rather detail analysis with geological information by using site reconnaissance result or existing geological information
- 3) Method Grade 3: detail analysis by using geological investigation result and numerical analysis

For evaluation of the slope failure, many characteristics are to be considered. Especially the following parameters are basic factors for stability of slope: scale of slope, shape of slope, geological condition, groundwater condition, type, shape or scale of failure, strength of ground.

There are varieties of slope characteristics in the Study area. It is difficult to take all these parameters into account for every slope and some statistical approach are considered. Therefore idea on combination of Grade 2 method and Grade 3 method is introduced.

“Average gradient method” is applied as Grade 2 method. This procedure considers average slope gradient within a 500m grid. The gradient is correlated to Japanese case study of slope stability during earthquake.

“Siyahi’s method” is applied as Grade 3 method. This procedure is based on stability calculation of circular arc failure. Various slope shape and soil strength are assumed as parameters and condition of minimum safety factor are determined.

Details are explained in the next section. Table 12.7.2 shows features of two methods.

Table 12.7.2 Two Types of Evaluation Method for Slope Stability

Method	Method Grade	Feature	Results	Parameter
Average Gradient	2	Evaluation of general slope stability in 500m grid	Possibility of slope failure	Slope gradient in average
Method of Siyahi	3	Evaluation of slope stability for steepest slope in 500m grid	Stable or unstable	Peak ground acceleration, Angle of internal friction, Steepest slope gradient

Siyahi’s method considers each slope conditions and detail distribution of earthquake ground motion. Topographical feature of the Study area is generally gentle. Once the steepest slope is selected, this does not represent general slope stability of each analysis unit. Therefore, some supplement idea to consider topographical feature is required. Average gradient of each analysis unit is another effective index. These two methods are combined and slope in failure potential in every 500m grids are evaluated. Figure 12.7.1 shows flow chart of slope stability analysis.

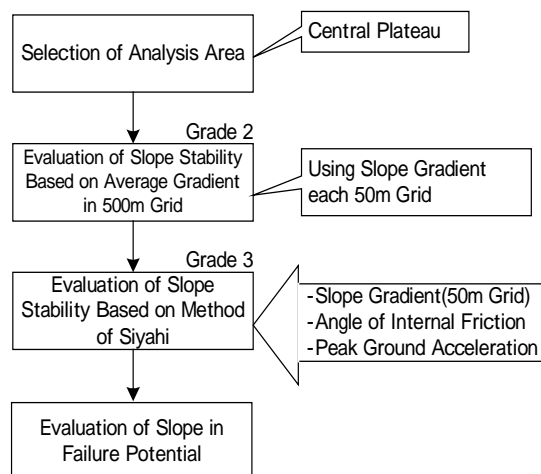


Figure 12.7.1 Flowchart of Slope Stability Analysis

2) Average Gradient Method

Matsuoka and Midorikawa (1995) proposed a procedure for evaluation of potential on earthquake induced slope failure. Average slope gradient are calculated using Japanese digital national land information. These are correlated to peak ground velocity, slope gradient, geomorphological unit and sediment type based on case histories of slope failure triggered by five Japanese earthquakes. Weight factor on each item are prepared and empirical equations for stability evaluation are proposed.

This procedure is basically grade 2 method therefore only factor “slope gradient” is picked up for consideration of topographical effect to slope stability. Weight factor is directory correlated to slope stability. (Table 12.7.3).

Table 12.7.3 Evaluation of Slope Stability Based on Average Gradient in 500m Grid

Slope Gradient (degree)	Weight *	Slope in Failure Potential **
16-	1.087	High
11-16	0.349	Relatively High
5-11	-0.211	Relatively Low
1-5	-0.067	Low
0.5-1	-0.280	
0-0.5	-1.002	

*Weight---Matsuoka and Midorikawa (1995)

**Evaluation Criteria are prepared by Study Team

3) Siyahi' Method

(1) Procedure

Siyahi and Ansal studied procedure of slope stability for microzonation purpose. This procedure is introduced in “Manual for Zonation on Seismic Geotechnical Hazards” by TC4, ISSMFE (1993) as Grade 3 method. Siyahi (1998) and Siyahi (2003) revised this procedure. The method originally proposed by Koppula (1984) was a pseudo-static evaluation of slope stability utilizing a seismic coefficient A to account for the earthquake induced horizontal forces. The variation in shear strength *s* with depth is assumed and potential failure surface is taken as a circular arc as shown in Figure 12.7.2.

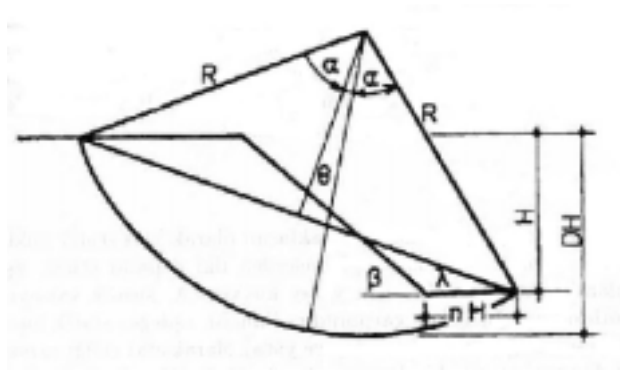


Figure 12.7.2 A Typical Section of Slope

Source: Siyahi (1998)

Parameters α , β , δ , and n are related to the geometry of the slope and configuration of sliding surface. Shear strength is defined as s . Then safety factor, F_s , can be defined as:

$$F_s = \frac{a_0}{\gamma} N_1 + \frac{c_0}{\gamma H} N_2$$

where

$$s = c_0 + a_0 z$$

$$N_1 = \frac{3(\alpha + \cot \delta - \alpha \cot \alpha \cot \delta)}{\sin^2 \alpha \times \sin^2 \delta (D_1 + D_2)} \quad N_2 = \frac{6\alpha}{\sin^2 \alpha \times \sin^2 \delta (D_1 + D_2)}$$

$$D_1 = 1 - 2 \cot^2 \beta - 3 \cot \alpha \cot \beta + 3 \cot \beta \cot \delta + 3 \cot \delta \cot \alpha - 6n \cot \beta - 6n^2 - 6n \cot \alpha + 6n \cot \delta$$

$$D_2 = A(\cot \beta + \cot^3 \beta + 3 \cot \alpha \cot^2 \delta - 3 \cot \alpha \cot \beta \cot \delta - 6n \cot \alpha \cot \delta)$$

If it is assumed that shear strength changes linear with depth, and $c_0=0$ for normally consolidated soil, then the shear strength of soils is represent as follows:

$$c_0 = 0$$

$$s = a_0 z$$

$$s = \sigma \tan \phi = \gamma z \tan \phi$$

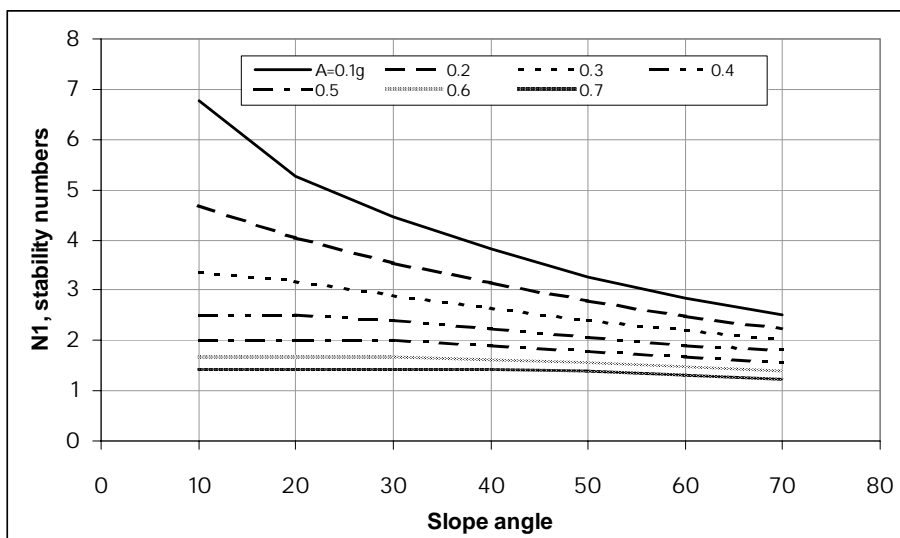
$$a_0 = \gamma \tan \phi$$

Then safety factor is calculated as

$$F_s = \frac{a_0}{\gamma} N_1 = \frac{\gamma \tan \phi}{\gamma} N_1 = N_1 \tan \phi$$

Thus the safety factor depends on the angle of shear strength and stability number N_1 representing the configuration of the slope and failure surface. The minimum value of the stability number are determined by carrying out a parametric study in terms of α , β , δ and n to find out the most critical failure surface as given in Figure 12.7.3. The variation of minimum N_1 can be expressed as a

function of β (slope gradient) and A (earthquake acceleration). In this study, β (slope gradient) is selected the most steep gradient, which is data of 50m grid, in 500m grid. And, A (earthquake acceleration) obtained from the result of the estimated ground motion is put into the calculation. Finally, slope stability condition is determined based on safety factor as shown in Table 12.7.4.



A: Acceleration

g: Gravitational acceleration

Figure 12.7.3 Relationship Between Slope Gradient, Seismic Coefficient and Minimum Shear Strength Stability Number

Source: Siyahi (2003)

Table 12.7.4 Evaluation of Slope Stability Based on Safety Factor

Safety Factor	Slope in Failure Potential*
$F_s < 1$	High
$1 \leq F_s \leq 1.5$	Moderate
$1.5 < F_s$	Low

*: "Manual for Zonation on Seismic Geotechnical Hazards"

(2) Limitation of the Procedure

Siyahi's procedure introduced idea for obtaining minimum safety factor for various shapes of failure surface and slope shape. And it assumes circular arc failure and normally consolidated soil. Only slope gradient and shear strength are required data for calculation. Furthermore, as results of the parametric approach, this procedure is considered to extend to not only circular surface failure but also another type of slope failure to some extent.

Slopes and failure types in the Study area are not always that of assumed in Siyahi’s procedure. However the characteristics of the procedure acts advantageous for considering the slope failure categorization.

4) Evaluation of Slope in Failure Potential

Table 12.7.5 shows final evaluation of slope in failure potential. Results of two methods are combined and final evaluation is prepared by matrix format. Basically Siyahi’s method gives higher priority.

Table 12.7.5 Matrix of Evaluation of Slope in Failure Potential

			Evaluation of Slope Stability Based on Average Slope Gradient			
			Slope in Failure Potential			
			Low	Relatively Low	Relatively High	High
Evaluation of Slope Stability Based on Method of Siyahi	Slope in Failure Potential	Low	Low			
		Moderate			Moderate	
		High			High	

12.7.3 Slope Stability

1) Setting of Properties

(1) Slope Gradient

Average slope gradient in 500m grids

Average slope gradient in 500m grid is calculated as average slope gradient of 50m grid in each 500m grid.

The Steepest slope gradient in 50m grids

The steepest slope gradient of 50m grid is selected.

(2) Peak Ground Acceleration

The peak ground acceleration in each 500m grid are allied for each scenario earthquake.

(3) Angle of Internal Friction

Angle of internal friction is the most important parameters for calculation. Available data are limited and do not cover for all the geological formation. Therefore the values are estimated considering existing reference, “Strength of Sliding Surface for Weathered Rocks”, quoted in

“Slope Stability and Stabilization Methods”, L. Abramson et al., 1996 (Table 12.7.6). The angle of internal friction was considered from 20 to 30 degree reference to the values of “Sedimentary rocks” in Table 12.7.6. Scenario earthquake Model 01 is recurrence of 1990 Luzon earthquake. There were no significant slope failures in Metropolitan Manila. Once less than 30 degrees are applied as angle of internal friction, slope in failure potential shows high in many places and this does not represent actual situation. On the other hand, over 30 degrees are applied, slope in failure potential shows low in many places and this is too much conservative evaluation. Finally 30 degrees is applied as angle of internal friction.

Table 12.7.6 Shear Strength of Residual Soils, Weathered Rocks and Related Minerals

Soil/Rock/Mineral Type	Degree of Weathering	Strength Parameters	
		Kg/cm ²	Degrees
Igneous Rocks			
Granite	Partly weathered (Zone IIB)		$\phi_f = 26 - 33$
Granite	Relatively sound (Zone III)		$\phi_f = 29 - 32$
Quartz diorite	Decomposed; sandy, silty	c=0.1	$\phi = 30 +$
Diorite	Weathered	c=0.3	$\phi = 22$
Rhyolite	Decomposed		$\phi' = 30$
Metamorphic Rocks			
Gneiss (micaceous)	Decomposed (Zone IB)	c = 0.3-0.6	$\phi = 23 - 37$
Gneiss	Decomposed (Zone IC)		$\phi = 18.5$
Gneiss	Decomposed (fault zone)	c=1.5	$\phi = 27$
	Much decomposed	c=4.0	$\phi = 29$
	Medium decomposed	c=8.5	$\phi = 35$
	Unweathered	c = 12.5	$\phi = 60$
Schist	Weathered (mica-schist soil)		$\phi = 24.5$
	Partly weathered	c=0.7	$\phi = 35$
Schist	Weathered		$\phi = 26 - 30$
Phyllite	Residual soil (Zone IC)	c=0	$\phi = 18 - 24$
Sedimentary rocks			
London clay	Weathered (brown)	c' = 1.2	$\phi' = 19 - 22$ $\phi_f = 14$
	Unweathered	c' = 0.9 - 1.8	$\phi' = 23 - 30$ $\phi_f = 18 - 24$
Keuper Marl	Highly weathered	c' < 0.1	$\phi' = 25 - 32$ $\phi_f = 18 - 24$
	Moderately weathered	c' < 0.1	$\phi' = 32 - 42$ $\phi_f = 22 - 29$
	Unweathered	c' < 0.3	$\phi' = 40$ $\phi_f = 23 - 32$
Shale	Shear zones		$\phi = 10 - 20$
Minerals			
Kaolinite	Minerals common in residual soils and rocks		$\phi_f = 12 - 22$
Illite			$\phi_f = 6.5 - 11.5$
Montmorillonite			$\phi_f = 40 - 11$

Source: Lee Abramson, Tom Lee, Suil Sharma, Glenn Boyce., 1996.